
TRANSDUCTIVE MAXIMUM MARGIN CLASSIFIER FOR FEW-SHOT LEARNING

Fei Pan

National Key Lab for Novel Software Technology
Nanjing University
Nanjing, 210023
felix.panf@outlook.com

Chunlei Xu

National Key Lab for Novel Software Technology
Nanjing University
Nanjing, 210023
xu.chunlei@outlook.com

Jie Guo

National Key Lab for Novel Software Technology
Nanjing University
Nanjing, 210023
guojie@nju.edu.cn

Yanwen Guo

National Key Lab for Novel Software Technology
Nanjing University
Nanjing, 210023
ywguo@nju.edu.cn

July 27, 2021

ABSTRACT

Few-shot learning aims to train a classifier that can generalize well when just a small number of labeled samples per class are given. We introduce Transductive Maximum Margin Classifier (TMMC) for few-shot learning. The basic idea of the classical maximum margin classifier is to solve an optimal prediction function that the corresponding separating hyperplane can correctly divide the training data and the resulting classifier has the largest geometric margin. In few-shot learning scenarios, the training samples are scarce, not enough to find a separating hyperplane with good generalization ability on unseen data. TMMC is constructed using a mixture of the labeled support set and the unlabeled query set in a given task. The unlabeled samples in the query set can adjust the separating hyperplane so that the prediction function is optimal on both the labeled and unlabeled samples. Furthermore, we leverage an efficient and effective quasi-Newton algorithm, the L-BFGS method to optimize TMMC. Experimental results on three standard few-shot learning benchmarks including miniImagenet, tieredImagenet and CUB suggest that our TMMC achieves state-of-the-art accuracies.

Keywords Few-shot learning, maximum margin classifier, separating hyperplane, L-BFGS

1 Introduction

In recent years, deep learning models have made remarkable progress in various vision and language tasks [1, 2, 3]. However, they have a common limitation, that training effective deep neural networks require a great number of labeled samples. When the training samples are insufficient, the trained model is prone to overfitting. Notably, humans are capable of learning from a small number of examples by leveraging past experiences. Inspired by this, few-shot learning aims to train a classifier that can generalize well when just a small number of labeled samples per class are given. In some situations, it is extremely difficult to obtain enough training examples, such as medical image processing, scarce plants and animals identification. Therefore, few-shot learning, which is designed to acquire a new visual concept through a small number of labeled samples, is attracting more and more research attentions.

In order to alleviate the overfitting problem caused by the inadequate labeled samples in few-shot learning, [4] proposed a episodic training strategy to learn over a few tasks and in each task the algorithm learns from a few labeled examples (the support set), which can be used to make predictions in the unlabeled examples (the query set). The intention of

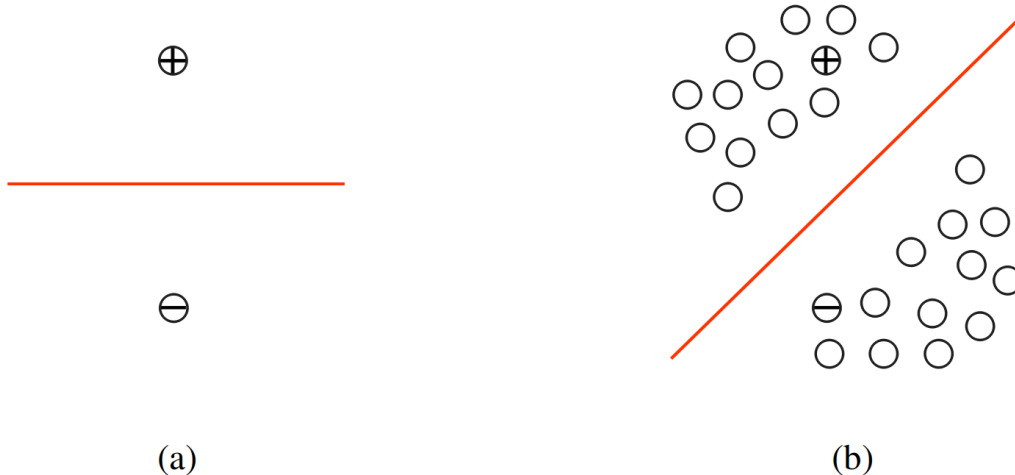


Figure 1: The symbols \oplus , \ominus , \circ in the figure denote the positive sample, the negative sample and the unlabeled sample, respectively. (a) An example of the 2-way 1-shot problem where there are totally 2 categories and each category consists of one sample in the support set. The maximum margin classifier would produce an optimal separating hyperplane as illustrated by the solid red line. (b) The unlabeled samples in the query set are involved in solving the optimal prediction function of the maximum margin classifier. We observe that the slope of the resulting separating hyperplane is quite different from that of (a). The solved optimal prediction function of (a) would produce a few misclassifications in the query set.

episodic training is that in real evaluation environment there are insufficient labeled examples in support sets and a few unlabeled examples in query set. The consistency between the training and evaluation stages reduces generalization errors by alleviating the distribution gap, so that this strategy has been adopted by the following works [5, 6, 7, 8, 9]. However, the episodic strategy cannot resolve the problem of learning from inadequate labeled data.

In this paper, we propose Transductive Maximum Margin Classifier (TMMC) for few-shot learning. The basic idea of the classical maximum margin classifier is to solve an optimal prediction function that the corresponding separating hyperplane can correctly divide the training data and the resulting classifier has the largest geometric margin. In few-shot learning scenarios, the training samples are scarce, not enough to find a separating hyperplane with good generalization ability on unseen data. TMMC is constructed using a mixture of labeled support set and unlabeled query set in a given task. Different from maximum margin classifier, the objective of TMMC also involves assigning labels to the query samples such that the best maximum margin classifier is constructed. Then at the evaluation stage, we estimate the prediction function on the query set by taking advantage of information from both the support set and the query set. The involvement of the query set in finding the optimal prediction function would yield improvement because of the insufficiency of the training points in the support set. The unlabeled samples in the query set can adjust the separating hyperplane so that the prediction function is optimal on both the labeled and unlabeled samples. Please refer to Figure 1 for an example that illustrates the research motivation of TMMC.

Our paper makes three main contributions. The first is that we propose Transductive Maximum Margin Classifier for few-shot learning. Our method minimize the prediction loss on both the labeled support set and the unlabeled query set and assign category labels to the samples in query set such that the best maximum margin classifier is constructed. The second contribution is that we leverage the one-vs-rest strategy to make our problem compatible with the binary classification model and use Platt scaling to transform the outputs of prediction function into a probability distribution over categories. The last is that we evaluate our method on three benchmark datasets for few-shot learning, namely miniImageNet, tieredImageNet and CUB. The experimental results show that our Transductive Maximum Margin Classifier achieves state-of-the-art results.

2 Related work

Few-Shot Learning is the bridge between artificial intelligence and human-like learning and the premise of cheap learning in industrial. There is a variety of works on Few-Shot Learning and a large body of approaches based on meta-learning. They obtain prior knowledge from tasks constructed from the base dataset, and then use the prior knowledge

to make predictions for the new tasks sampled from test dataset. These approaches can be broadly categorized into five categories by prior knowledge representations.

Metric-based methods [10, 4, 11] learn the similarity measure of samples and predict the labels of query samples by measuring distances. Koch et al. [10] employ a Siamese network to measure the similarity between query samples and support samples. Snell et al. [11] use the class prototypes which are the means of embeddings of support samples from the corresponding categories and rank the Euclidean distances of the query sample to each prototypes. Triantafillou et al. [12] also employ the unlabeled examples when producing prototypes.

Memory-based methods [13, 4, 14] employ the key-value memory architectures. Santoro et al. [13] introduced MANN which originally uses memory networks for few shot learning based on NTM [15] to store sample features and labels in a one-to-one correspondence form and update elements with the least recently used strategy. MetaNet [14] stores model parameters in memory which is the fast weight for each support sample to help query sample get relevant fast weights, and updates parameters across tasks.

Optimization-based methods [5, 6, 16, 17, 18, 19] optimize the parameters of the base network by fast gradient-based adaptation, which results in task-special weights called the fast weights. MAML[5] learns good initialization of parameters in the model. The learned parameters may not perform well on the tasks, but using these parameters as a starting point, it would learn new tasks effectively and efficiently. Instead of adapting the high-dimensional model parameters through back propagation as in [5], [17, 18, 19, 7] perform adaptation in latent space which is more generalizable to new tasks. LEO [7] learns the model parameters of an encoder and an decoder and makes adaptations in low-dimensional latent space.

Generation-based methods [20, 21, 22, 23, 8] produce parameters of neural networks based on labeled samples of tasks. Munkhdalai et al. [20] produce the activations of additive biases by adaptive neurons. They only produce a part of model parameters to adjust the network for tasks rather than encoding the tasks. LGM-Net [8] directly generates the parameters of the whole feature extraction network, using of the latent representation of support set to generate weights.

Transductive methods [24, 25, 26, 27, 9, 28] construct the models using both the labeled and unlabeled samples, making full use of the task information. The models of transductive methods make predictions on the unlabeled query samples of a single few-shot task at once, instead of processing one sample at a time as in inductive methods. TPN [24] learns to propagate labels by label propagation, which leverages an extra network to get the weight matrix between pairs of samples. CAN-T [25] utilizes attention mechanisms to calculate the cross attention map between the support set and the query set, making the extracted features more discriminant.

Several recent works deal with the problem of few-shot learning without taking advantage of episodic-learning. In the training stage, they train an general classification network on the base dataset which will be used as a feature extractor in the evaluation stage. SimpleShot [29] shows that a simple nearest-neighbor classifier with feature transformations and L2-normalization leads to competitive few-shot learning results. Then LaplacianShot [30] propose a transductive Laplacian-regularized inference based on the same setting as in [29] and minimize a quadratic binary-assignment function to encourage similar samples to be assigned with the same labels. In contrast to their approaches, our method leverages the unlabeled samples in the query set to adjust the separating hyperplane so that the prediction function of the maximum margin classifier is optimal on both the labeled and unlabeled samples.

3 Transductive Maximum Margin Classifier

3.1 Problem Setting

In the few-shot classification setting, we use the episodic formulation from [4] where each episode mimics a task. Tasks are sampled from three datasets with non-overlapping classes: base dataset \mathcal{D}_{base} , validation dataset $\mathcal{D}_{validation}$ and test dataset \mathcal{D}_{test} . The goal is to train a model using \mathcal{D}_{base} , which can generalize well in \mathcal{D}_{test} and the set of $\mathcal{D}_{validation}$ is used to tune the hyper-parameters. In a N -way K -shot task, we randomly sample N categories from the dataset and K samples from each category to construct the support set $\mathcal{S}' = \{(z_i, y_i)\}_{i=1}^{NK}$. The model is evaluated in the query set $\mathcal{Q}' = \{(z_i, y_i)\}_{i=1}^{NQ}$ where Q samples are provided for each category.

3.2 Proposed method

We begin by introducing the hinge loss function: $l(u) = \max(0, 1 - u)$. Support Vector Machines is the corresponding maximum margin classifier, which solves:

$$\underset{f \in \mathcal{H}}{\text{minimize}} \lambda \|f\|_{\mathcal{H}}^2 + \frac{1}{n} \sum_{i=1}^n l(y_i f(\mathbf{x}_i)), \quad (1)$$

where f lies in a Reproducing Kernel Hilbert Space \mathcal{H} , $y_i \in \{-1, +1\}$, and $\lambda > 0$ is a hyper-parameter.

We first train a base-learner using deep neural networks g_θ with parameter θ using the set \mathcal{D}_{base} . The dimension of the extracted features using g_θ is D . Then we sample a batch of N -way K -shot tasks from \mathcal{D}_{test} . Each task involves a support set $\mathcal{S} = \{(\mathbf{x}_i, y_i) | \mathbf{x}_i = g_\theta(\mathbf{z}_i), (\mathbf{z}_i, y_i) \in \mathcal{S}', i = 1, \dots, NK\}$ and a query set $\mathcal{Q} = \{(\mathbf{x}_i, y_i) | \mathbf{x}_i = g_\theta(\mathbf{z}_i), (\mathbf{z}_i, y_i) \in \mathcal{Q}', i = 1, \dots, NQ\}$.

We use the one-vs-rest strategy to make our problem compatible with the binary classification model. For each category $c \in \{1, \dots, N\}$, we modify the value of y_i in the set \mathcal{S} to $+1$ if $y_i = c$ and -1 otherwise to obtain a new vector

$$\mathbf{y}^c = [y_i^c | y_i^c = 1 \text{ if } y_i = c \text{ else } -1, (\mathbf{x}_i, y_i) \in \mathcal{S}, i = 1, \dots, NK]^T \in R^{NK}. \quad (2)$$

Due to the introduction of the one-vs-rest strategy, the training samples of each category become unbalanced. So we assign weights to all samples in the support set and adjust weights inversely proportional to category frequencies: $\mathbf{w}^c = [w_1^c, w_2^c, \dots, w_{NK}^c]^T$. Besides, we define the following matrices:

$$\mathbf{X}_{\mathcal{S}} = [\mathbf{x}_i | (\mathbf{x}_i, y_i) \in \mathcal{S}, i = 1, \dots, NK] \triangleq [\mathbf{x}_1, \dots, \mathbf{x}_{NK}] \in R^{D \times NK} \quad (3)$$

$$\mathbf{X}_{\mathcal{Q}} = [\mathbf{x}_i | (\mathbf{x}_i, y_i) \in \mathcal{Q}, i = 1, \dots, NQ] \triangleq [\mathbf{x}_{NK+1}, \dots, \mathbf{x}_{NK+NQ}] \in R^{D \times NQ} \quad (4)$$

Then we take advantage of the unlabeled samples in $\mathbf{X}_{\mathcal{Q}}$ to get more accurate prediction functions [31, 32]. Specifically, we are intended to find the optimal $f^c \in \mathcal{H}$ and the label vector $\mathbf{y}^{c'} = [y_1^{c'}, \dots, y_{NQ}^{c'}]^T$ by the following optimization problem:

$$\underset{f^c \in \mathcal{H}, \mathbf{y}^{c'}}{\text{minimize}} \lambda_1 \|f^c\|_{\mathcal{H}}^2 + \frac{1}{NK} \sum_{i=1}^{NK} w_i^c l(y_i^c f(\mathbf{x}_i)) + \lambda_2 \frac{1}{NQ} \sum_{j=1}^{NQ} l(y_j^{c'} f(\mathbf{x}_{NK+j})), \quad (5)$$

where $\lambda_1, \lambda_2 > 0$ are hyper-parameters. The third term in Equation 5 is designed to find the optimal label vector $\mathbf{y}^{c'}$ together with the optimal prediction function, which renders this problem difficult to optimize.

By the representer theorem [33], the solution satisfies

$$f^{c*}(\mathbf{x}) = \sum_{i=1}^{NK+NQ} \alpha_i^{c*} k(\mathbf{x}_i, \mathbf{x}), \quad (6)$$

where the function k is the reproducing kernel of \mathcal{H} .

From [34], the optimal value of $y_j^{c'}$ equals 1 if $f(\mathbf{x}_{NK+j}) \geq 0$ and -1 otherwise. By introducing the vectors $\alpha^c = [\alpha_1^c, \dots, \alpha_{NK+NQ}^c]^T$, α^{c*} solves

$$\begin{aligned} \arg \min_{\alpha^c} \lambda_1 (\alpha^c)^T \mathbf{K} \alpha^c + \frac{1}{NK} \sum_{i=1}^{NK} w_i^c \max(0, 1 - y_i^c f(\mathbf{x}_i)) \\ + \lambda_2 \frac{1}{NQ} \sum_{j=1}^{NQ} \max(0, 1 - |f(\mathbf{x}_{NK+j})|), \end{aligned} \quad (7)$$

where \mathbf{K} is a matrix with elements $K_{ij} = k(\mathbf{x}_i, \mathbf{x}_j)$, $i, j \in \{1, 2, \dots, NK + NQ\}$.

Obviously, Equation 7 is non-convex and non-differentiable. In order to optimize it efficiently, we replace the non-differentiable parts of Equation 7 with their differentiable surrogates. More precisely, in Equation 7, the term of $\max(0, 1 - y_i^c f(\mathbf{x}_i))$ is replaced by $\frac{1}{\gamma_1} \log(1 + \exp(\gamma_1(1 - y_i^c f(\mathbf{x}_i))))$ [35] and the term of $\max(0, 1 - |f(\mathbf{x}_{NK+j})|)$ is replaced by $\exp(-\gamma_2 f(\mathbf{x}_{NK+j})^2)$ [34]. $\gamma_1, \gamma_2 \geq 0$ are hyper-parameters. As a consequence, we obtain the following optimization problem:

$$\begin{aligned} \arg \min_{\alpha^c} F(\alpha^c) = \lambda_1 (\alpha^c)^T \mathbf{K} \alpha^c + \frac{1}{NK} \sum_{i=1}^{NK} \frac{w_i^c}{\gamma_1} \log(1 + \exp(\gamma_1(1 - y_i^c f(\mathbf{x}_i)))) \\ + \lambda_2 \frac{1}{NQ} \sum_{j=1}^{NQ} \exp(-\gamma_2 f(\mathbf{x}_{NK+j})^2). \end{aligned} \quad (8)$$

The gradient of $F(\alpha^c)$ w.r.t α^c is

$$\nabla_{\alpha^c} F(\alpha^c) = 2\lambda_1 \mathbf{K} \alpha^c + \mathbf{K} \mathbf{t}, \quad (9)$$

Algorithm 1: Transductive Maximum Margin Classifier

Input: base dataset \mathcal{D}_{base} , and test dataset \mathcal{D}_{test} ; feature extractor g_{θ} using deep neural networks with parameter θ ; hyper-parameters: $\lambda_1, \gamma_1, \gamma_2$ and \mathbf{v}_{λ_2} .

Optimize θ using \mathcal{D}_{base} ;

Sample batch of N -way K -shot tasks $\{\mathcal{T}_i\}_{i=1}^M$ from \mathcal{D}_{test} ;

for each \mathcal{T}_i **do**

Fetch the support set $\mathcal{S} = \{(\mathbf{x}_i, y_i)\}_{i=1}^{NK}$ and the query set $\mathcal{Q} = \{(\mathbf{x}_i, y_i)\}_{i=1}^{NQ}$;

for c in $\{1, \dots, N\}$ **do**

Obtain the vectors $\mathbf{y}^c, \mathbf{w}^c$ and $\mathbf{x}_i, i = 1, \dots, NK + NQ$;

for λ_2 in $\{0, v_1, v_2, \dots\}$ **do**

Initialize the inverse Hessian approximation \mathbf{H}^0 ;

Initialize α_0^c if λ_2 equals 0;

$k = 0$;

while not converged do

Obtain $\nabla_{\alpha^c} F(\alpha_k^c)$ using Equation 9;

Calculate $\mathbf{d}_k = -\mathbf{H}^k \nabla_{\alpha^c} F(\alpha_k^c)$;

Find the appropriate step size t_k by line search and update $\mathbf{a}_{k+1}^c = \alpha_k^c + t_k \mathbf{d}_k$;

Update the inverse Hessian approximation \mathbf{H}^{k+1} using L-BFGS;

$k = k + 1$;

end

$\alpha_0^c = \alpha_k^c$;

end

Acquire $p_j^c, j = 1, \dots, NQ$ using Platt Scaling;

end

Obtain the predicted labels $y_j = \arg \max_c p_j^c, j = 1, \dots, NQ$.

end

where $\mathbf{t} \in R^{NK+NQ}$ is a vector with elements

$$t_i = \begin{cases} -\frac{w_i^c y_i^c \exp(\gamma_1(1 - y_i^c f(\mathbf{x}_i)))}{NK(1 + \exp(\gamma_1(1 - y_i^c f(\mathbf{x}_i))))} & i \leq NK, \\ -\frac{2\gamma_2 \lambda_2 f(\mathbf{x}_i) \exp(-\gamma_2 f(\mathbf{x}_i)^2)}{NQ} & otherwise. \end{cases} \quad (10)$$

3.3 Optimization

In order to optimize the proposed model efficiently, we use the BFGS algorithm which can generate an approximate Hessian matrix at each step with a small computational cost [32]. The iterative sequence generated by using the approximate matrix instead of the Hessian matrix still has the property of superlinear convergence.

Given an initial $\alpha_0^c \in R^{NK+NQ}$, the BFGS algorithm calculates the sequence $\alpha_1^c, \dots, \alpha_k^c, \alpha_{k+1}^c$ iteratively until convergence via

$$\mathbf{a}_{k+1}^c = \alpha_k^c + t_k \mathbf{d}_k \quad (11)$$

where t_k is the stepsize and the direction $\mathbf{d}_k = -\mathbf{H}^k \nabla_{\alpha^c} F(\alpha_k^c)$.

The update of the inverse Hessian approximation is given by [36]:

$$\mathbf{H}^{k+1} = (I - \rho_k \mathbf{s}_k \mathbf{w}_k^T) \mathbf{H}^k (I - \rho_k \mathbf{w}_k \mathbf{s}_k^T) + \rho_k \mathbf{s}_k \mathbf{s}_k^T \quad (12)$$

where $\rho_k = (\mathbf{w}_k^T \mathbf{s}_k)^{-1}$, $\mathbf{w}_k = \nabla_{\alpha^c} F(\alpha_{k+1}^c) - \nabla_{\alpha^c} F(\alpha_k^c)$ and $\mathbf{s}_k = \alpha_{k+1}^c - \alpha_k^c$.

Although the BFGS method overcomes the difficulty of calculating the Hessian matrix, it still cannot be applied to large-scale optimization problems. Generally speaking, the inverse Hessian approximation \mathbf{H}^k is a dense matrix, and storing the dense matrix consumes $O(n^2)$ memory, which is obviously impossible for large-scale problems. In this paper, we use the limited memory version of BFGS method (L-BFGS) to reduce the computational cost and memory storage.

When the value of λ_2 equals 0 in Equation 8, it corresponds to a special form of maximum margin classifier. In order to adjust the separating hyperplane of the maximum margin classifier, we initially set the value of λ_2 to 0 and increase its value gradually. This way of updating the value of λ_2 results in a sequence $v_{\lambda_2} = \{0, v_1, v_2, \dots\}$.

When the iteration of λ_2 ends and the termination criteria of L-BFGS methods is satisfied, we get the predicted values on the vector \mathbf{x}_i using Equation 6: $e_i^c = f^{c*}(\mathbf{x}_i), i = 1, \dots, NK + NQ$. Then, we use Platt scaling [37] to transform the outputs of Equation 6 into a probability distribution over categories. Specifically, we firstly let s_i^c equals 0 if $y_i^c = -1$ and 1 otherwise; then we leverage the data pairs $\{(e_i^c, s_i^c)\}_{i=1}^{NK}$ to train a logistic regression model r^c . The predicted probabilities on the query set are given by $p_j^c = r^c(e_{j+NK}^c), j = 1, \dots, NQ$. Finally, we obtain the predicted labels on the query set $y_j = \arg \max_c p_j^c, j = 1, \dots, NQ$. The overall method is summarized in Algorithm 1.

4 Experiment

4.1 Datasets

We experiment on three benchmarks for few-shot classification: miniImagenet, tieredImagenet and CUB-200-2011.

miniImagenet. The miniImagenet dataset [4] is constructed from the ImageNet [38] dataset, which is established to facilitate the study of visual recognition and is the largest image recognition database in the world. The miniImagenet consists of 100 classes and 600 images of size 84×84 per class. We follow the split employed by previous works, dividing the dataset into base, validation and test sets, with 64, 16, and 20 categories respectively.

tieredImagenet. The tieredImagenet [12] is a larger subset sampled from ImageNet, consisting of 608 classes. It divides classes into broader categories that correspond to nodes at the higher levels in the ImageNet hierarchy. There are 34 big categories and 10 to 30 classes per category. Following the split proposed by Triantafillou et al. [12], there are 20 categories with 351 classes, 6 categories consisting of 97 classes and 8 categories containing 160 classes, for base, validation and test datasets.

CUB-200-2011. The CUB-200-2011 [39] is a fine-grained bird image classification dataset, which is the benchmark in the research of fine-grained classification and recognition. We split it into 100 basic classes, 50 validation classes and 50 test classes with about 50 samples per classes and resize the images to 84×84 pixels as miniImagenet, following previous works [30].

4.2 Network Models

We evaluate TMMC on three different network architectures as the feature extractor g_θ . **ResNet-18** [40] is a variant of the standard 18-layer architecture with 8 basic residual blocks, where the first two down-sampling layers are removed and the kernel size in the first convolutional layer is modified from 7×7 to 3×3 . **WRN** [41] adds more convolutional layers and feature planes to widen the residual blocks. Following the architecture used in LEO [7], we set the number of convolutional layers to 28 and set the widening factor to 10. **DenseNet** [42] is based on the standard 121-layer architecture with 58 dense blocks, leaving out the first two down-sampling operations and setting the kernel size in the first convolutional layer to 3×3 .

4.3 Implementation Details

Model training: We train the base-learner neural network using the cross-entropy loss on the base dataset and set the label-smoothing parameter to 0.1. The models are optimized using SGD, with early stopping and the learning rate initialized to 0.1. During training, we use the data augmentation strategy which includes random cropping, color jitter and random horizontal flipping and the images are resized to 84×84 . The networks are trained on four GeForce GTX 1080Ti GPUs.

Feature transformation: During evaluation on a task sampled from test dataset, we first compute the mean of the features, $\bar{\mathbf{x}} = \frac{1}{|S|+|Q|} \sum_{\mathbf{x} \in S \cup Q} \mathbf{x}$, and then center the image features by subtracting this mean as $\mathbf{x} := \mathbf{x} - \bar{\mathbf{x}}$. At last image features are normalized by L2 normalization: $\mathbf{x} := \frac{\mathbf{x}}{\|\mathbf{x}\|_2}$.

Experimental settings: For simplicity, we keep the hyper-parameters of our method fixed across all the experiments. The hyper-parameters are obtained using the validation set of miniImagenet and are set as follows: $\lambda_1 = 0.02, \gamma_1 = 20.0, \gamma_2 = 2.0$. The sequence $v_{\lambda_2} = \{0, 0.00001, 0.001, 0.1, 1.0\}$. Besides, we use the linear kernel function in all experiments: $k(\mathbf{x}_i, \mathbf{x}_j) = \mathbf{x}_i^T \mathbf{x}_j, i, j \in \{1, 2, \dots, NK + NQ\}$

Evaluation Protocol: Following [7, 29], we evaluate on 5-way 1-shot and 5-way 5-shot tasks by randomly sampling 10,000 tasks from the test dataset. Each N-way K-shot task has N classes and K images per class in support set and 15

Table 1: Averaged accuracy (in %) on miniImageNet and tieredImageNet. The values represent the averaged accuracies in 10,000 episodes from the test dataset with 95% confidence intervals. The best results are reported in bold font.

Methods	Network	miniImageNet		tieredImageNet	
		5-way 1-shot	5-way 5-shot	5-way 1-shot	5-way 5-shot
MAML[5]	ResNet-18	49.61±0.92	65.72±0.77	-	-
Chen et al.[43]	ResNet-18	51.87±0.77	75.68±0.63	-	-
RelationNet[44]	ResNet-18	52.48±0.86	69.83±0.68	-	-
MatchingNet[4]	ResNet-18	52.91±0.88	68.88±0.69	-	-
Gidaris et al.[21]	ResNet-15	55.45±0.89	70.13±0.68	-	-
ProtoNet[11]	ResNet-18	54.16±0.82	73.68±0.65	-	-
SNAIL[19]	ResNet-15	55.71±0.99	68.88±0.92	-	-
Bauer et al.[45]	ResNet-34	56.30±0.40	73.90±0.30	-	-
AdaCNN[46]	ResNet-15	56.88±0.62	71.94±0.57	-	-
TADAM[47]	ResNet-15	58.50±0.30	76.70±0.30	-	-
CAML[48]	ResNet-12	59.23±0.99	72.35±0.71	-	-
TPN[24]	ResNet-12	59.46	75.64	-	-
TEAM[49]	ResNet-18	60.07	75.90	-	-
MTL[50]	ResNet-18	61.20±1.80	75.50±0.80	-	-
VariationalFSL[51]	ResNet-18	61.23±0.26	77.69±0.17	-	-
Transductive tuning[52]	ResNet-12	62.35±0.66	74.53±0.54	-	-
MetaoptNet[53]	ResNet-18	62.64±0.61	78.63±0.46	65.99±0.72	81.56±0.53
SimpleShot[29]	ResNet-18	63.10±0.20	79.92±0.14	69.68±0.22	84.56±0.16
CAN+T[25]	ResNet-12	67.19±0.55	80.64±0.35	73.21±0.58	84.93±0.38
LaplacianShot[30]	ResNet-18	72.11 ±0.19	82.31±0.14	78.98±0.21	86.39±0.16
TMMC (ours)	ResNet-18	71.92±0.26	82.48 ±0.15	79.21 ±0.26	87.09 ±0.15
Qiao[22]	WRN	59.60±0.41	73.74±0.19	-	-
LEO[7]	WRN	61.76±0.08	77.59±0.12	66.33±0.05	81.44±0.09
ProtoNet[11]	WRN	62.60±0.20	79.97±0.14	-	-
CC+rot[54]	WRN	62.93±0.45	79.87±0.33	70.53±0.51	84.98±0.36
MatchingNet[4]	WRN	64.03±0.20	76.32±0.16	-	-
FEAT[55]	WRN	65.10±0.20	81.11±0.14	70.41±0.23	84.38±0.16
Transductive tuning[52]	WRN	65.73±0.68	78.40±0.52	73.34±0.71	85.50±0.50
SimpleShot[29]	WRN	65.87±0.20	82.09±0.14	70.90±0.22	85.76±0.15
SIB[56]	WRN	70.0±0.6	79.2±0.4	-	-
BD-CSPN[57]	WRN	70.31±0.93	81.89±0.60	78.74±0.95	86.92±0.63
LaplacianShot[30]	WRN	74.86 ±0.19	84.13±0.14	80.18±0.21	87.56±0.15
TMMC (ours)	WRN	74.74±0.24	84.71 ±0.14	80.76 ±0.25	88.35 ±0.15
SimpleShot[29]	DenseNet	65.77±0.19	82.23±0.13	71.20±0.22	86.33±0.15
LaplacianShot[30]	DenseNet	75.57 ±0.19	84.72±0.13	80.30±0.22	87.93±0.15
TMMC (ours)	DenseNet	75.31±0.25	85.10 ±0.13	82.22 ±0.25	89.40 ±0.14

images per class in query set. We report the averaged accuracy of 10,000 tasks with the 95% confidence interval in the following experiments.

4.4 Results

We first compare our TMMC on miniImageNet and tieredImageNet with state-of-the-art methods in 5-way 1-shot and 5-way 5-shot experimental settings of few-shot learning. As shown in Table 1, TMMC outperforms state-of-the-art methods except for the 5-way 1-shot setting in miniImageNet where the accuracies are slightly lower than that of LaplacianShot [30]. It’s worth noting that our method outperforms all other methods in the tieredImageNet dataset across different network models and the largest performance gains over LaplacianShot are obtained by using the DenseNet models.

Then we report the experimental results on CUB dataset in Table 2. Following [43], we also conduct a cross-domain experiment from miniImageNet to CUB. Specifically, we train a ResNet-18 model on the miniImageNet base dataset and employ the trained model to extract features in the CUB test dataset. As we can see, TMMC outperforms the other methods by large margins in the 5-way 5-shot cross-domain setting.

Table 2: Averaged accuracy in CUB and cross-domain results from miniImageNet \rightarrow CUB.

Methods	Network	CUB		miniImageNet \rightarrow CUB	
		5-way 1-shot	5-way 5-shot	5-way 1-shot	5-way 5-shot
MatchingNet[4]	ResNet-18	73.49	84.45	-	53.07
MAML[5]	ResNet-18	68.42	83.47	-	51.34
ProtoNet[11]	ResNet-18	72.99	86.64	-	62.02
RelationNet[44]	ResNet-18	68.58	84.05	-	57.71
Chen et al.[43]	ResNet-18	67.02	83.58	-	65.57
SimpleShot[29]	ResNet-18	70.28	86.37	48.56	65.63
LaplacianShot[30]	ResNet-18	80.96	88.68	55.46	66.33
TMMC (ours)	ResNet-18	81.08	89.07	54.57	69.65

Table 3: Ablation study of the involvement of the unlabeled samples in the query set in solving the optimal prediction function of the maximum margin classifier.

Network	Methods	miniImageNet		tieredImageNet	
		5-way 1-shot	5-way 5-shot	5-way 1-shot	5-way 5-shot
ResNet-18	MMC	64.15	79.79	71.83	85.18
ResNet-18	TMMC	71.92	82.48	79.21	87.09
WRN	MMC	67.21	82.36	73.16	86.37
WRN	TMMC	74.74	84.71	80.76	88.35
DenseNet	MMC	67.11	82.68	73.81	87.36
DenseNet	TMMC	75.31	85.10	82.22	89.40

The inference run-time per few-shot learning task in the 5-way 5-shot setting on mini-ImageNet dataset with the WRN backbone is about 1.0 seconds on the Intel Core i9-9900X CPU. In algorithm 1, the most time is spent traversing the sequence $v_{\lambda_2} = \{0, 0.00001, 0.001, 0.1, 1.0\}$ and the categories which take the value from the collection $\{1, \dots, 5\}$.

4.5 Ablation study

In order to evaluate the effectiveness of the proposed method, we set the value of λ_2 to 0 in Equation 8 which is equivalent to the setting that the sequence $v_{\lambda_2} = \{0\}$. In this case, the additional unlabeled samples from the query set are removed from solving the maximum margin classifier. The hyper-parameters are set as follows: $\lambda_1 = 0.02, \gamma_1 = 20.0$. In this experiment, the parameter γ_2 has no effect on the results, so we omit its value here. We call the resulting model Maximum Margin Classifier (MMC) in the following.

Table 3 summarizes the results in this experimental setting compared with TMMC. We observe that TMMC outperforms MMC by more than 7% in 5-way 1-shot setting and 2% to 3% in 5-way 5-shot setting. The gains are consistent across different network models. As a consequence, we conclude that the involvement of the unlabeled samples in the query set in solving the optimal prediction function of the maximum margin classifier plays a significant role in achieving better few-shot learning results.

5 Conclusions

In this paper, we proposed Transductive Maximum Margin Classifier (TMMC) for few-shot learning. Our method utilized the unlabeled query set for transductive inference. Different from the classical maximum margin classifier, TMMC also assigns labels to the query samples such that the best maximum margin classifier is constructed. By gradually increasing the weight of the loss function evaluated at the query set, we adjust the separating hyperplane so that the prediction function is optimal on both the labeled and unlabeled samples. We conducted extensive experiments on the datasets including miniImageNet, tieredImageNet and CUB where we obtained state-of-the-art results.

In future work, we are going to extend the formulation of Transductive Maximum Margin Classifier to solve the multi-class problem by considering all categories at once. In doing so, the inference time will be greatly reduced, because we do not need to traverse the categories.

References

- [1] Kaiming He, Xiangyu Zhang, Shaoqing Ren, and Jian Sun. Deep residual learning for image recognition. In *CVPR*, 2016.
- [2] Shaoqing Ren, Kaiming He, Ross Girshick, and Jian Sun. Faster r-cnn: Towards real-time object detection with region proposal networks. In *NeurIPS*, 2015.
- [3] Jacob Devlin, MingWei Chang, Kenton Lee, and Kristina Toutanova. Bert: Pre-training of deep bidirectional transformers for language understanding. In *arXiv*, 2018.
- [4] Oriol Vinyals, Charles Blundell, Tim Lillicrap, Koray Kavukcuoglu, and Daan Wierstra. Matching networks for one shot learning. In *NeurIPS*, 2016.
- [5] Chelsea Finn, Pieter Abbeel, and Sergey Levine. Model-agnostic meta-learning for fast adaptation of deep networks. In *ICML*, 2017.
- [6] Alex Nichol, Joshua Achiam, and John Schulman. On first-order meta-learning algorithms. *arXiv*, 2018.
- [7] Andrei A. Rusu, Dushyant Rao, Jakub Sygnowski, Oriol Vinyals, Razvan Pascanu, Simon Osindero, and Raia Hadsell. Meta-learning with latent embedding optimization. In *ICLR*, 2019.
- [8] Huai-Yu Li, Weiming Dong, Xing Mei, Chongyang Ma, Feiyue Huang, and Bao-Gang Hu. Lgm-net: Learning to generate matching networks for few-shot learning. In *ICML*, 2019.
- [9] Jongmin Kim, Taesup Kim, Sungwoong Kim, and Chang D. Yoo. Edge-labeling graph neural network for few-shot learning. In *CVPR*, 2019.
- [10] Gregory Koch, Richard Zemel, and Ruslan Salakhutdinov. Siamese neural networks for one-shot image recognition. 2015.
- [11] Jake Snell, Kevin Swersky, and Richard S. Zemel. Prototypical networks for few-shot learning. In *NeurIPS*, 2017.
- [12] Eleni Triantafillou, Hugo Larochelle, Jake Snell, Josh Tenenbaum, Kevin Jordan Swersky, Mengye Ren, Richard Zemel, and Sachin Ravi. Meta-learning for semi-supervised few-shot classification. In *ICLR*, 2018.
- [13] Adam Santoro, Sergey Bartunov, Matthew Botvinick, Daan Wierstra, and Timothy P. Lillicrap. Meta-learning with memory-augmented neural networks. In *ICML*, 2016.
- [14] Tsendsuren Munkhdalai and Hong Yu. Meta networks. In *ICML*, 2017.
- [15] Alex Graves, Greg Wayne, and Ivo Danihelka. Neural turing machines. (*10 Dec 2014*), 2014.
- [16] Zhenguo Li, Fengwei Zhou, Fei Chen, and Hang Li. Meta-sgd: Learning to learn quickly for few shot learning. *arXiv*, 2017.
- [17] Yoonho Lee and Seungjin Choi. Gradient-based meta-learning with learned layerwise metric and subspace. In Jennifer G. Dy and Andreas Krause, editors, *ICML*, 2018.
- [18] Fengwei Zhou, Bin Wu, and Zhenguo Li. Deep meta-learning: Learning to learn in the concept space. *arXiv*, 2018.
- [19] Nikhil Mishra, Mostafa Rohaninejad, Xi Chen, and Pieter Abbeel. A simple neural attentive meta-learner. In *ICLR*, 2018.
- [20] Tsendsuren Munkhdalai, Xingdi Yuan, Soroush Mehri, Tong Wang, and Adam Trischler. Learning rapid-temporal adaptations. *arXiv*, 2017.
- [21] Spyros Gidaris and Nikos Komodakis. Dynamic few-shot visual learning without forgetting. In *CVPR*, 2018.
- [22] Siyuan Qiao, Chenxi Liu, Wei Shen, and Alan L. Yuille. Few-shot image recognition by predicting parameters from activations. In *CVPR*, 2018.
- [23] Marta Garnelo, Dan Rosenbaum, Christopher Maddison, Tiago Ramalho, David Saxton, Murray Shanahan, Yee Whye Teh, Danilo Jimenez Rezende, and S. M. Ali Eslami. Conditional neural processes. In *ICML*, 2018.
- [24] Yanbin Liu, Juho Lee, Minseop Park, Saehoon Kim, Eunho Yang, Sung Ju Hwang, and Yi Yang. Learning to propagate labels: Transductive propagation network for few-shot learning. In *ICLR*, 2019.
- [25] Ruibing Hou, Hong Chang, Bingpeng Ma, Shiguang Shan, and Xilin Chen. Cross attention network for few-shot classification. In *NeurIPS*, 2019.
- [26] Guneet Singh Dhillon, Pratik Chaudhari, Avinash Ravichandran, and Stefano Soatto. A baseline for few-shot image classification. In *ICLR*, 2020.

- [27] Xu Hu, Pablo Moreno, Yang Xiao, Xi Shen, Guillaume Obozinski, and Neil Lawrence. Empirical bayes transductive meta-learning with synthetic gradients. In *ICLR*, 2020.
- [28] Limeng Qiao, Yemin Shi, Jia Li, Yonghong Tian, Tiejun Huang, and Yaowei Wang. Transductive episodic-wise adaptive metric for few-shot learning. In *ICCV*, 2019.
- [29] Yan Wang, Wei-Lun Chao, Kilian Q. Weinberger, and Laurens van der Maaten. Simpleshot: Revisiting nearest-neighbor classification for few-shot learning. *arXiv*, 2019.
- [30] Imtiaz Masud Ziko, Jose Dolz, Eric Granger, , and Ismail Ben Ayed. Laplacian regularized few-shot learning. In *ICML*, 2020.
- [31] Kristin P Bennett and Ayhan Demiriz. Semi-supervised support vector machines. In *NeurIPS*, 1999.
- [32] F. Gieseke, A. Airola, T. Pahikkala, and O. Kramer. Sparse quasi-newton optimization for semi-supervised support vector machines. In *ICPRAM*, 2012.
- [33] Bernhard Schölkopf, Ralf Herbrich, and Alex J Smola. A generalized representer theorem. computational learning theory. In *Lecture Notes in Computer Science*, 2001.
- [34] O. Chapelle and A. Zien. Semi-supervised classification by low density separation. In *AISTATS*, 2005.
- [35] T. Zhang and F. J. Oles. Text categorization based on regularized linear classification methods. In *Information Retrieval*, 2001.
- [36] S.J. Wright J. Nocedal. Numerical optimization. In *Springer Science Business Media*, 2006.
- [37] John Platt. Probabilistic outputs for support vector machines and comparisons to regularized likelihood methods. In *Advances in Large Margin Classifiers*, 1999.
- [38] Jia Deng, Wei Dong, Richard Socher, Li-Jia Li, Kai Li, and Fei-Fei Li. Imagenet: A large-scale hierarchical image database. In *CVPR*, 2009.
- [39] C. Wah, S. Branson, P. Welinder, P. Perona, and S. Belongie. The Caltech-UCSD Birds-200-2011 Dataset. Technical report, 2011.
- [40] Kaiming He, Xiangyu Zhang, Shaoqing Ren, and Jian Sun. Deep residual learning for image recognition. In *CVPR*, 2016.
- [41] Sergey Zagoruyko and Nikos Komodakis. Wide residual networks. In *BMVC*, 2016.
- [42] G. Huang, Z. Liu, Vdm Laurens, and K. Q. Weinberger. Densely connected convolutional networks. In *IEEE Computer Society*, 2016.
- [43] Wei-Yu Chen, Yen-Cheng Liu, Zsolt Kira, Yu-Chiang Frank Wang, and Jia-Bin Huang. A closer look at few-shot classification. In *ICLR*, 2019.
- [44] Flood Sung, Yongxin Yang, Li Zhang, Tao Xiang, Philip H. S. Torr, and Timothy M. Hospedales. Learning to compare: Relation network for few-shot learning. In *CVPR*, 2018.
- [45] Matthias Bauer, Mateo Rojas-Carulla, Jakub Bartłomiej Swiatkowski, Bernhard Schölkopf, and Richard E. Turner. Discriminative k-shot learning using probabilistic models. *arXiv*, 2017.
- [46] Tsendsuren Munkhdalai, Xingdi Yuan, Soroush Mehri, and Adam Trischler. Rapid adaptation with conditionally shifted neurons. In *ICML*, 2018.
- [47] Boris N. Oreshkin, Pau Rodríguez López, and Alexandre Lacoste. TADAM: task dependent adaptive metric for improved few-shot learning. In *NeurIPS*, 2018.
- [48] Xiang Jiang, Mohammad Havaei, Farshid Varno, Gabriel Chartrand, Nicolas Chapados, and Stan Matwin. Learning to learn with conditional class dependencies. In *ICLR*, 2019.
- [49] L. Qiao, Y. Shi, J. Li, Y. Tian, T. Huang, and Y. Wang. Transductive episodic-wise adaptive metric for few-shot learning. In *ICCV*, 2019.
- [50] Qianru Sun, Yaoyao Liu, Tat-Seng Chua, and Bernt Schiele. Meta-transfer learning for few-shot learning. In *CVPR*, 2019.
- [51] Jian Zhang, Chenglong Zhao, Bingbing Ni, Minghao Xu, and Xiaokang Yang. Variational few-shot learning. In *ICCV*, 2019.
- [52] Guneet Singh Dhillon, Pratik Chaudhari, Avinash Ravichandran, and Stefano Soatto. A baseline for few-shot image classification. In *ICLR*, 2020.
- [53] Kwonjoon Lee, Subhansu Maji, Avinash Ravichandran, and Stefano Soatto. Meta-learning with differentiable convex optimization. In *CVPR*, 2019.

- [54] Spyros Gidaris, Andrei Bursuc, Nikos Komodakis, Patrick Pérez, and Matthieu Cord. Boosting few-shot visual learning with self-supervision. In *ICCV*, 2019.
- [55] Han-Jia Ye, Hexiang Hu, De-Chuan Zhan, and Fei Sha. Few-shot learning via embedding adaptation with set-to-set functions. In *CVPR*, 2020.
- [56] Shell Xu Hu, Pablo Garcia Moreno, Yang Xiao, Xi Shen, Guillaume Obozinski, Neil D. Lawrence, and Andreas C. Damianou. Empirical bayes transductive meta-learning with synthetic gradients. In *ICLR*, 2020.
- [57] Jinlu Liu, Liang Song, and Yongqiang Qin. Prototype rectification for few-shot learning. In *ECCV*, 2020.